first, second and third steps were similar to those of g1. After the third step, the tines were again closed within the shaft and then fully expanded.[18]

Power was first applied at 30 W and then increased at 10-W increments every minute in each step to a maximum of 120 W. The power was fixed once it reached 120 W. The necessary electric power and tissue impedance were recorded every 15 s. The procedure was applied continuously until a rise in impedance (caused by coagulation necrosis) with a corresponding drop in delivered power (a phenomenon called "roll-off"). The energy requirement for ablation was integration of the electric power (W) over the ablation time (s), which could be calculated approximately by summing a product of 15 (s) and the electric power measured every 15 s.

Image analysis

Tumor size, location and vascularity were evaluated before RFA using contrast-enhanced CT or MRI. Dynamic CT scans were performed using nonionic contrast material unless the patient was allergic to the iodine medium, for whom MRI was performed. Dynamic CT consisted of the arterial phase (30-s delay), hepatic portal phase (60-s delay) and hepatic venous phase (120-s delay) with slice thickness of 5 mm after the start of injection, respectively. Contrast-enhanced MRI was performed with i.v. injection of contrast material Gd-EOB-DTPA (EOB-MRI). Dynamic MRI consisted of the arterial phase (30-s delay), hepatic portal phase (60-s delay) and hepatic venous phase (120- and 180-s delay) with a thickness of 5 mm and hepatocyte-specific phase (>20 min delay) with a thickness of 3 mm. The tumor was appraised as "hypervascular" when it was stained denser on the arterial phase image compared to the surrounding liver parenchyma.

One to three days after the treatment, the size and shape of the RF-induced lesion was evaluated by measuring three perpendicular dimensions of portal phase images of the contrast-enhanced CT or MRI, calculating the hypothetical volume of the ablated zone. In cases in which CT/MRI images were taken along the needle trace and those perpendicular to the needle, we measured the length of the ablated area along the needle tract and the diameter of the area perpendicular to it.

Statistical analysis

The duration of ablation, required energy and the size of the ablated lesions were compared between the two groups using the Mann–Whitney *U*-test. All values were expressed as median. A *P*-value less than 0.05 denoted the presence of a statistically significant difference.

RESULTS

Ablation time and required energy

ROLL-OFF WAS achieved at each step of ablation in all 30 RFA procedures. Table 2 shows the time to reach roll-off at each step and total ablation time in the two groups. These results indicate that the durations of the first step, second step and third step were similar for groups 1 and 2 ($P = 0.356$, $= 0.457$ and $= 0.590$, respectively), while that of the fourth step and total session were longer for group 2 than group 1 ($P < 0.001$ and <0.001, respectively). The energy required for one procedure was 18.1 kJ (range, 10.7–31.3) and 59.9 kJ (range, 35.1–119.5) for groups 1 and 2, respectively, indicating more energy requirement for group 2 than group 1 ($P < 0.0001$).

Needle expansion

Figure 1 depicts CT images showing the tines in the tumor in the final step; Figure 1(a,b) shows a cross-

Table 2 Comparison of ablation time (in min/s) and radio frequency-induced areas between groups 1 and 2

	Group 1	Group 2	*P*
Duration of the first step	1′ 53″ (0′ 54″–3′ 43″)	2′ 37″ (1′ 00″–4′ 34″)	0.356
Second step	2′ 14″ (0′ 40″–4′ 57″)	2′ 21″ (0′ 16″–3′ 35″)	0.457
Third step	1′ 26″ (0′ 52″–2′ 46″)	1′ 30″ (0′ 57″–4′ 38″)	0.590
Fourth step	1′ 36″ (1′ 02″–3′ 55″)	9′ 20″ (6′ 39″–17′ 13″)	<0.001
Total ablation time	7′ 36″ (5′ 07″–10′ 13″)	15′ 07″ (11′ 22″–25′ 05″)	<0.001
Required energy for ablation, kJ	18.1 (10.7–31.3)	59.9 (35.1–119.5)	<0.001
Long diameter, mm	30 (21–37)	37 (31–60)	0.001
Short diameter, mm	26 (16–32)	28 (25–39)	0.045
Axial diameter, mm	35 (20–45)	40 (30–50)	0.018

Data are median (range).

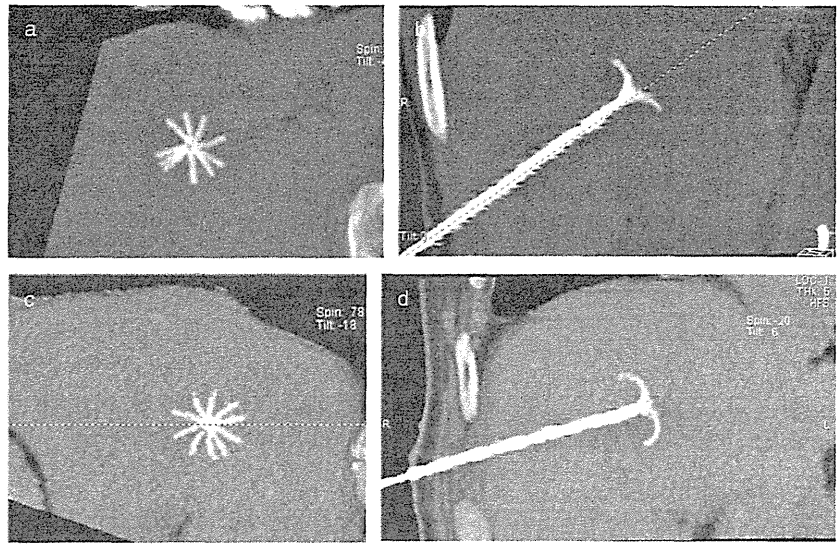

Figure 1 Electrode tines in the final step. (a,b) Tines are uniformly and fully expanded. (c,d) Tines are irregularly and insufficiently expand.

section perpendicular to the needle axis and that along the axis of group 1. Figure 1(c,d) shows those of group 2. All tines are almost uniformly extended as shown in Figure 1(c), while two tines remained attached to each other in Figure 1(a). We checked for needle expansion during RFA in six cases; three cases of group 1 and three cases of group 2. No uniform expansion was detected in any of the cases (0%) of group 1 and 2 cases (67%) of group 2, while irregular expansion was identified in three cases (100%) of group 1 and one case (33%) of group 2. Furthermore, the extent of the expansion at the final step was larger in Figure 1(b) than in (d).

Size and shape of ablated tissue

Table 2 also shows the long and short diameters of the axial cross-section and axial length of the ablated lesions measured on CT images in the two groups. The long diameter was 30 mm (range, 21–37) in group 1 and 37 mm (range, 31–60) in group 2. The short diameter was 26 mm (range, 16–32) in group 1 and 28 mm (range, 25–39) in group 2. The axial length was 35 mm (range, 20–45) in group 1 and 40 mm (range, 30–50) in group 2. All three diameters of group 2 were significantly longer than those of group 1.

In six patients, we reconstructed the post-RFA CT images to show the length of the ablated zone along the shaft and its vertical diameter (Fig. 2). When the tines were uniformly expanded as shown in Figure 1(c), the cross-sectional shape of the ablated zone perpendicular to the axis was nearly circular (Fig. 2c). The zone was more irregular when the tines were non-uniformly separated (see Fig. 1a); the cross-section was also irregular in shape similar to Figure 1(a). In the former case, the ablated zone along the shaft was near-oval in shape with the short axis equivalent to the shaft (Fig. 2d), while the shape was parachute-like or was irregularly shaped sometimes in the latter case (Fig. 2b).

Comparison of the long and short diameters in patients with cirrhosis and without cirrhosis showed that neither the long axis nor the short axis were significantly different; the long diameters in patients with cirrhosis and without cirrhosis were 33 mm (range, 21–53) and 32 mm (range, 25–60), respectively ($P = 0.451$). The short diameter in patients with cirrhosis and without cirrhosis were 27 mm (range, 16–39) and 27 mm (range, 21–36), respectively ($P = 0.983$).

Complications

We did not encounter any episodes of heat injury to adjacent organs, skin burn, symptomatic pleural effusion, intrahepatic abscess, intraperitoneal bleeding or renal failure in either group.

DISCUSSION

RADIOFREQUENCY ABLATION THERAPY is one the curative therapies for HCC measuring less than 30 mm in diameter, whereas surgical resection is the only curative treatment for HCC of more than 30 mm and less than 50 mm in diameter. However, surgical resection cannot be performed in patients with severe liver dysfunction or severe vascular invasion. In Japan,

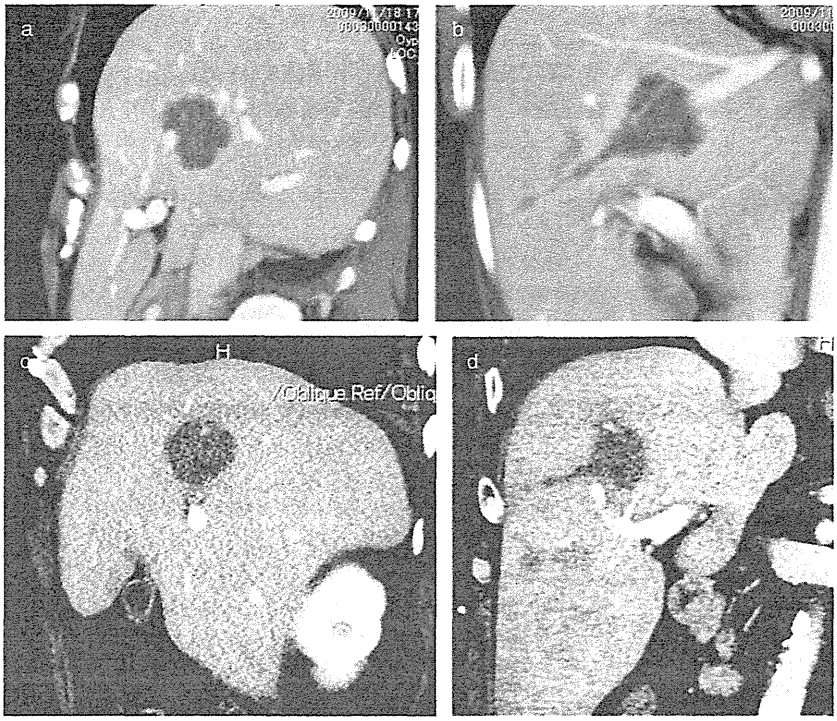

Figure 2 Dynamic computed tomography images of post-radiofrequency ablation lesions produced by the conventional procedure (group 1) and the new procedure (group 2). (a) The shape of the lesion perpendicular to the axis in group 1 is irregular. (b) The shape of the lesion along the axis in group 1 is parachute-like. (c) The shape perpendicular to the axis in group 2 is nearly circular. (d) The shape along the axis in group 2 is ellipsoid.

the Japan Society of Hepatology issued consensus-based HCC treatment guidelines in 2010, which include a HCC treatment algorithm. In this algorithm, resection can be selected with a patient with liver function Child–Pugh class A/B and without vascular invasion or with Vp1 or 2.[19] Thus, a technique that widens the RF-ablated area can improve, at least theoretically, the survival of cirrhotic patients with HCC over 30 mm in diameter.

The shape of the ablated zone depends on the needle type.[3] For example, the path along the shaft is longer than the transverse diameter when using the cool-tip electrode (cool-tip RF system), shorter when using the expandable needle of the RTC system and compatible with each other when using the LeVeen needle (RITA system). The shorter path is less disadvantageous than the shorter perpendicular diameter, because the ablated zone along with the needle trace can be enlarged by repeating the procedure as the needle is extracted while that perpendicular to the tract cannot be enlarged during one insertion. Although it is often difficult to achieve roll-off during a single-step full expansion procedure using the LeVeen needle, our stepwise procedure[13] overcomes this difficulty and produces an oval ablation zone similar to the single-step procedure. The more slender expandable LeVeen Superslim needle is easier and safer to insert into the liver. However, it is easier to deform during insertion and hardly extend as expected; it cannot be fully extended when expanded slowly. This is because the shaft is pushed back as the electrode is inserted toward the liver. To overcome this inconvenience, we designed a new technique, full re-expansion after stepwise extension, which allows a sharper and definite expansion of the slim needle to full length.

We have demonstrated in our previous experimental study,[18] using the pig liver *in vivo*, that the new extension procedure for the expandable needle allows coagulation of a larger and more oval lesion even when using the slim needle. One of the differences between the pig experimental study and the clinical study is that RFA is applied in patients with HCC who have chronically damaged livers. The results showed that the new procedure can also produce a larger ablated zone of which the long axis is perpendicular to the needle shaft compared to that of the conventional procedure in chronically damaged livers; the size of the ablated zone was independent of the liver architecture and liver fibrosis.

The ablation times in this clinical study were similar to those of the experimental studies; the duration of the first, second and third steps were similar in groups 1 and

2, while those of the fourth step and total session were longer in group 2 than group 1. The energy required for one procedure was larger in group 2 than in group 1. The roll-off phenomenon represents marked increase in tissue impedance due to coagulation necrosis. In other words, once the roll-off occurs, the tissue in contact with tines is isolated. Thus, the additional electric current and energy cannot be introduced when the positions of tines are kept in the same position just after the roll-off. After the humors soaks into necrotic tissue from outside normal liver tissue, the additional electric current and electric power can be input. But because the penetrating humor is of small amount, the input electric power shortly enables humors to evaporate and roll-off may occur again soon. Therefore, the second ablation using conventional procedure cannot prominently enlarge the ablated area over 30 mm of diameter which the RTC system exhibits. The shape of ablated area also cannot be clearly changed. A few papers reported the results of double roll-off ablation procedure without change in probe positions,[20–22] showing that this double roll-off procedure cannot ablate the zone bigger than the diameter of the fully expanded needle. The ablation zone was approximately 3 cm with a 14-G LeVeen needle 35 mm in diameter.[20] Even with a 12-tine LeVeen needle 40 mm in diameter, the diameter perpendicular to the axis was 34.4 ± 2.1 mm and the axial diameter was 31.0 ± 6.2 mm.[21] The difference of energy between group 1 and group 2 is due to that of ablated volume because the required energy for ablation per volume is almost identical.[18]

We suggested in our previous study[18] that the smaller ablation zone produced by the conventional stepwise method was due to the facts that the hooks of the Super-Slim needles hardly extended to full extension during the slow insertion because the shaft was pushed back as the electrode was inserted toward the liver and that the tanned tumor or parenchymal tissues were removed from the surface of the multiple tines when they were once enclosed within the shaft in the new method, resulting in a better outcome of RF ablation. Our study identified another reason for the difference in the size of the ablated zone; the tines were extended separately in more cases of group 2, while some tines remained attached to each other in more cases of group 1 than of group 2. It is possible that this is because the tines gathered in one direction in the first step as the tip of the needle shaft was diagonally cut and the direction of the extension of each tine could not be reset in the conventional procedure. When all tines were separately extended, the cross-section was nearly circular and its size was larger due to the better RFA, compared with the irregular shape and smaller size when two or three tines remained attached to each other. In addition, the median of the long axis with the new method is much larger not only than that with the conventional method using a slim needle but also that of the conventional method with an old needle of 15-G diameter.[3,13] It means this method using a slim needle is most appropriate when we want the largest ablated zone among various methods: the conventional method using a slim needle, that using a 15-G needle and the ablation using cool-tip needle.

In conclusion, the new extension procedure using the slim expandable needle allows coagulation of the largest area among various procedures using various types of needles. Additionally, the two kinds of stepwise procedures allow the selection of a more suitable procedure based on the tumor size and shape in each RFA.

REFERENCES

1 Bruix J, Sherman M. Management of hepatocellular carcinoma. *Hepatology* 2005; **42**: 1208–36.
2 Ikeda K, Kobayashi M, Saitoh S *et al.* Cost-effectiveness of radiofrequency ablation and surgical therapy for small hepatocellular carcinoma of 3 cm or less in diameter. *Hepatol Res* 2005; **33**: 241–9.
3 Mulier S, Ni Y, Miao Y *et al.* Size and geometry of hepatic radiofrequency lesions. *Eur J Surg Oncol* 2003; **29**: 867–78.
4 Livraghi T, Goldberg SN, Monti F *et al.* Saline-enhanced radio-frequency tissue ablation in the treatment of liver metastasis. *Radiology* 1997; **202**: 205–10.
5 Burdio F, Guemes A, Burdio JM *et al.* Large hepatic ablation with bipolar saline-enhanced radiofrequency: an experimental study in vivo porcine liver with a novel approach. *J Surg Res* 2003; **110**: 193–201.
6 Kurokohchi K, Watanabe S, Masaki T *et al.* Combined use of percutaneous ethanol injection and radiofrequency ablation for the effective treatment of hepatocellular carcinoma. *Int J Oncol* 2002; **21**: 841–6.
7 Watanabe S, Kurokohchi K, Masaki T *et al.* Enlargement of thermal ablation zone by the combination of ethanol injection and radiofrequency ablation in excised bovine liver. *Int J Oncol* 2004; **24**: 279–84.
8 Kurokohchi K, Masaki T, Miyauchi Y *et al.* Efficacy of combination therapies of percutaneous ethanol-lipiodol injection and radiofrequency ablation. *Int J Oncol* 2004; **25**: 1737–43.
9 Sugimoto K, Morimoto M, Shirato K *et al.* Radiofrequency ablation in a pig liver model: effect of transcatheter arterial embolization on coagulation diameter and histological characteristics. *Hepatol Res* 2002; **24**: 164–73.
10 Yamasaki T, Kurosawa F, Shirahashi H, Kusano N, Hironaka K, Okita K. Percutaneous radiofrequency abla-

tion therapy with combined angiography and computed tomography assistance for patients with hepatocellular carcinoma. *Cancer* 2001; **91**: 1342–8.
11 Kobayashi M, Ikeda K, Kawamura Y *et al.* Randomized controlled trial for the efficacy of hepatic arterial occlusion during radiofrequency ablation for small hepatocellular carcinoma-Direct ablative effects and a long-term outcome. *Liver Int* 2007; **27**: 353–9.
12 Chinn SB, Lee FT Jr, Kennedy GD *et al.* Effect of vascular occlusion on radiofrequency ablation of the liver. *AJR Am J Roentgenol* 2001; **176**: 789–95.
13 Kobayashi M, Ikeda K, Someya T *et al.* Stepwise hook extension technique for radiofrequency ablation therapy of hepatocellular carcinoma. *Oncology* 2002; **63**: 139–44.
14 Nakamuta M, Kohjima M, Morizono S *et al.* Comparison of tissue pressure and ablation time between LeVeen and cool-tip needle methods. *Comp Hepatol* 2006; **5**: 10.
15 Kotoh K, Nakamuta M, Morizono M *et al.* A multi-step, incremental expansion method for radio frequency ablation: optimization of the procedure to prevent increases in intra-tumor pressure and to reduce the ablation time. *Liver Int* 2005; **25**: 542–7.
16 Kotoh K, Enjoji M, Arimura E *et al.* Scattered and rapid intrahepatic recurrences after radio frequency ablation for hepatocellular carcinoma. *World J Gastroenterol* 2005; **11**: 6828–32.
17 Hirakawa M, Ikeda K, Kawamura Y *et al.* Lipiodol and dye at the site of ablation decreases during RFA. *Intervirology* 2008; **51**: 362–8.
18 Hirakawa M, Ikeda K, Kawamura Y *et al.* New ablation procedure for a radiofrequency liver tissue coagulation system using an expandable needle. *Liver Int* 2007; **28**: 214–9.
19 Yamashita T, Kaneko S. Treatment strategies for hepatocellular carcinoma in Japan. *Hepatol Res* 2012; (in press).
20 McGahan JP, Dodd GD 3rd. Radiofrequency ablation of the liver: current status. *AJR Am J Roentgenol* 2001; **176**: 3–16.
21 Pereira PL, Trubenbach J, Schenk M *et al.* Radiofrequency ablation: in vivo comparison of four commercially available devices in pig livers. *Radiology* 2004; **232**: 482–90.
22 Arata MA, Nisenbaum HL, Clark TW, Soulen MC. Percutaneous radiofrequency ablation of liver tumors with the LeVeen probe: is roll-off predictive of response? *J Vasc Interv Radiol* 2001; **12**: 455–8.

Hepatol Int (2013) 7:850–858
DOI 10.1007/s12072-012-9419-7

Three-dimensional magnetic resonance imaging for stringent diagnosis of advanced fibrosis associated with nonalcoholic steatohepatitis

Yusuke Kawamura · Satoshi Saitoh · Yasuji Arase · Kenji Ikeda · Taito Fukushima · Tasuku Hara · Yuya Seko · Tetsuya Hosaka · Masahiro Kobayashi · Hitomi Sezaki · Norio Akuta · Fumitaka Suzuki · Yoshiyuki Suzuki · Kei Fukuzawa · Yusuke Hamada · Junji Takahashi · Mariko Kobayashi · Hiromitsu Kumada

Received: 19 September 2012 / Accepted: 8 December 2012 / Published online: 30 January 2013

Abstract
Background The definitive diagnosis of nonalcoholic steatohepatitis (NASH) is currently based on histopathological assessment. This study aimed to elucidate the utility of a novel noninvasive method, three-dimensional magnetic resonance imaging (3D-MRI), for diagnosing advanced fibrosis in patients with NASH, using histopathological diagnosis as the reference standard.
Methods This retrospective study included 30 consecutive patients who had been diagnosed with NASH by histopathology and had undergone 3D-MRI before biopsy. 3D-MRI provided a three-dimensional reconstruction of the liver from contrast-enhanced hepatobiliary phase MR images. In the present study, histopathological advanced fibrosis was defined as stage 3 and 4 NASH. Advanced fibrosis, diagnosed by 3D-MRI, was considered to be diffuse irregularity of the entire surface of the liver. The diagnostic features of 3D-MRI and the noninvasive evaluation systems (APRI, FIB-4 index, and BARD score) for identifying advanced and nonadvanced fibrosis of NASH were determined and compared.
Results Nine (30 %) of the 30 study patients were diagnosed histopathologically with advanced fibrosis, and 11 (37 %) of 30 patients were diagnosed with advanced fibrosis using 3D-MRI. The sensitivity, specificity, positive predictive value (PPV), and negative predictive value (NPV) of 3D-MRI for diagnosing advanced fibrosis were 100, 90, 82, and 100 %, respectively. The sensitivities of APRI, the FIB-4 index, and BARD score ranged from 78 to 89 %, the specificities from 71 to 90 %, the PPVs from 54 to 78 %, and the NPVs from 88 to 94 %.
Conclusion Compared with the common noninvasive methods for diagnosing advanced fibrosis associated with NASH, 3D-MRI was more accurate.

Keywords Nonalcoholic fatty liver disease · Nonalcoholic steatohepatitis · Advanced fibrosis · 3D-MRI · Virtual MR-laparoscopy

Y. Kawamura (✉) · S. Saitoh · Y. Arase · K. Ikeda · T. Fukushima · T. Hara · Y. Seko · T. Hosaka · M. Kobayashi · H. Sezaki · N. Akuta · F. Suzuki · Y. Suzuki · H. Kumada
Department of Hepatology, Toranomon Hospital, 2-2-2, Toranomon, Minato-ku, Tokyo 105-8470, Japan
e-mail: k-yusuke@toranomon.gr.jp

Y. Kawamura · S. Saitoh · Y. Arase · K. Ikeda · T. Fukushima · T. Hara · Y. Seko · T. Hosaka · M. Kobayashi · H. Sezaki · N. Akuta · F. Suzuki · Y. Suzuki · K. Fukuzawa · Y. Hamada · J. Takahashi · M. Kobayashi · H. Kumada
Okinaka Memorial Institute for Medical Research, Toranomon Hospital, Tokyo, Japan

K. Fukuzawa · Y. Hamada · J. Takahashi
Department of Radiology, Toranomon Hospital, Tokyo, Japan

M. Kobayashi
Research Institute for Hepatology, Toranomon Hospital, Tokyo, Japan

Introduction

Nonalcoholic fatty liver disease (NAFLD) is a common cause of chronic liver disease in Western countries [1–4], and recently it has become common in many Asian nations [5, 6]. In particular, patients with nonalcoholic steatohepatitis (NASH), a subcategory of NAFLD, are at an increased risk for developing hepatocellular carcinoma [7]. Like patients with viral hepatitis, NAFLD patients with advanced fibrosis have an increased risk of developing hepatocellular carcinoma [8–10]. Currently, NASH can be diagnosed only by histopathology. Usually, chronic liver

depression), (2) partially irregular (several interconnected depressions on the surface, mainly in the left lobe of the liver, with rippled or speckled appearance), and (3) diffusely irregular (including diffuse small irregularities or large irregularities with areas of nodularity).

MR image acquisition and 3D reconstruction of the liver were performed by three expert radiologic technologists. The 3D-MR images were evaluated for degree of fibrosis (nonadvanced or advanced fibrosis) by a conference of three expert hepatologists who were blinded to the pathological results. Each hepatologist had 10 or more years of experience performing conventional diagnostic laparoscopy to assess chronic liver disease.

Definition of advanced fibrosis according to APRI, FIB-4 index, BARD score, and 3D-MRI

Advanced fibrosis was defined as follows: (1) APRI >0.98, (2) FIB-4 index >2.67, (3) BARD score = 2–4, and (4) image from 3D-MRI showing diffuse irregularity of the surface of the liver (including diffuse small irregularities or large irregularities with areas of nodularity).

Statistical analysis

Differences in demographic features, laboratory data, and the features of liver biopsy specimens between patients with advanced fibrosis versus patients with nonadvanced fibrosis were analyzed by the Fisher's exact test and Mann-Whitney *U* test. The sensitivity, specificity, PPV, and NPV for identifying advanced and nonadvanced fibrosis were determined for each evaluation system (APRI, FIB-4 index, and BARD score) and 3D-MRI. A p value of <0.05 was considered statistically significant. Data analysis was performed using the Statistical Package for Social Sciences, version 11.0 (SPSS Inc., Chicago, IL, USA).

Results

Clinical and demographic features of patients

Table 1 summarizes the demographic and clinical profiles of the 30 study patients. The patients with advanced

Table 1 Clinical and demographic features of patients with nonalcoholic steatohepatitis who underwent three-dimensional magnetic resonance imaging

	All patients	Nonadvanced fibrosis (stage 1–2) $n = 21$	Advanced fibrosis (stage 3–4) $n = 9$	p value
Gender (M:F)	22:8	17:4	5:4	0.195
Age (years)[a]	59.5 (29–80)	47 (29–73)	63 (51–80)	0.032
Body mass index (kg/m^2)[a]	25.8 (20.8–37.9)	25.4 (20.9–35.1)	26.2 (20.8–37.9)	0.533
Albumin (g/dl)[a]	4.2 (3.6–4.7)	4.2 (3.8–4.7)	3.9 (3.6–4.4)	0.086
Total bilirubin (mg/dl)[a]	0.9 (0.4–1.5)	0.8 (0.4–1.2)	0.9 (0.5–1.5)	0.150
AST (IU/l)[a]	48 (18–198)	41 (18–198)	48 (29–150)	0.422
ALT (IU/l)[a]	76.5 (22–275)	83 (22–275)	45 (22–194)	0.077
γ-GTP (IU/l)[a]	57.5 (15–502)	67 (15–502)	54 (34–125)	0.929
Platelet count (× 10^3/μl)[a]	196 (65–318)	215 (104–318)	181 (65–207)	0.002
Hyaluronic acid (μg/l)	28 (4–196)	21 (4–83)	127 (47–196)	<0.001
Diabetes mellitus (yes/no)	6:24	4:17	2:7	1.000
Uric acid (mg/dl)[a]	6.4 (3.6–9.6)	6.7 (4.7–8.9)	5.3 (3.6–9.6)	0.104
Total cholesterol (mg/dl)[a]	193.5 (94–265)	206 (94–265)	172 (107–223)	0.070
Triglyceride (mg/dl)[a]	144.5 (38–355)	157 (38–276)	140 (40–355)	0.965
LDL-cholesterol (mg/dl)[a]	104.5 (24–177)	113 (24–177)	85 (28–124)	0.025
HDL-cholesterol (mg/dl)[a]	45 (22–76)	45 (28–76)	41 (22–59)	0.304
Needle biopsy specimens of the liver ($n = 29$)[b]				
		$n = 21$	$n = 8$	
Length of specimens (mm)	15 (9–27)	15 (9–27)	20.5 (13–26)	0.024
Number of portal areas	6 (2–21)	5 (2–21)	9.5 (6–12)	0.006

ALT alanine aminotransferase, *AST* aspartate aminotransferase, *γ-GTP* gamma-glutamyl transpeptidase, *HDL* high-density lipoprotein, *LDH* lactate dehydrogenase, *LDL* low-density lipoprotein

[a] Expressed as median (minimum, maximum)

[b] One patient who underwent surgical resection for hepatocellular carcinoma was excluded from quality evaluation of the needle biopsy specimens

fibrosis were significantly older, and they had significantly lower platelet counts, lower low-density lipoprotein-cholesterol levels, and higher hyaluronic acid levels compared with the patients with nonadvanced fibrosis. With regard to the characterization of the needle biopsy specimens (one patient undergoing surgical resection for hepatocellular carcinoma was excluded from quality evaluation of the needle biopsy specimens), the patients with advanced fibrosis had significantly larger specimens and higher numbers of portal areas.

3D-MRI and histological NASH stage

Figure 1a–d shows 3D-MRI figures that corresponded to the different histological NASH stages. These 3D-MRI figures demonstrate that in addition to altered shape of the liver, the irregularities on the surface of the liver gradually extended from the lateral segment to the right lobe. There were nine patients with the Fig. 1a pattern, and all (100 %) were histopathologically diagnosed with NASH stage 1. Of ten patients with the Fig. 1b pattern, five (50 %) were diagnosed with NASH stage 1 and five with NASH stage 2. Of 9 patients with the Fig. 1c pattern, 5 (56 %) were diagnosed with NASH stage 3, 2 (22 %) with NASH stage 4, and 2 with NASH stage 1. Two patients (7 %) had the Fig. 1d pattern, and both were diagnosed with NASH stage 4. Diffuse irregularities of the entire surface of the liver were characteristic of patients with NASH stage 3 and 4; therefore, we designated 3D-MR images showing irregularities of the entire surface of the liver as advanced fibrosis (Fig. 1c, d). A total of 11 (37 %) of 30 patients were diagnosed with advanced fibrosis from the figures obtained by 3D-MRI.

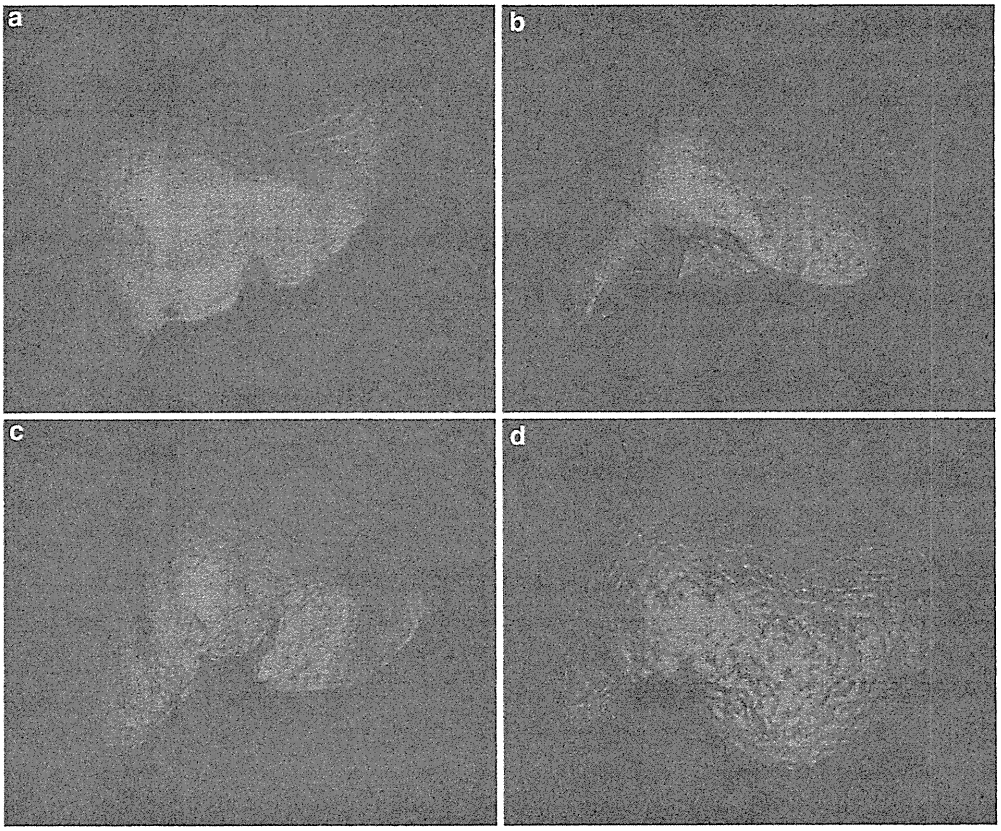

Fig. 1 **a** Three-dimensional magnetic resonance image of nonadvanced liver fibrosis in nonalcoholic steatohepatitis (NASH), stage 1, showing a smooth liver surface and enlarged lateral segment. **b** Image of nonadvanced fibrosis, NASH stage 2, showing localized small irregularities of the surface of the liver and an enlarged lateral segment. **c** Image of advanced fibrosis, NASH stage 3, showing diffuse small irregularities of the surface of the liver and enlarged lateral segment. **d** Image of advanced fibrosis, NASH stage 4, showing diffuse large irregularities of the surface of the liver, an enlarged lateral segment, and atrophic right lobe

Figures 2 and 3 are conventional laparoscopic images of livers of patients with advanced fibrosis (NASH stage 3 and 4, respectively). Figure 2a, b shows diffuse small irregularities of the entire surface of the liver, and the surface of the left lobe (Fig. 2b) has diffuse small irregularities and a large nodular area. The histological diagnosis of this patient was NASH stage 3, and the 3D-MR image of this patient is also shown in Fig. 1c. Figure 3a, b shows diffuse bilobular large irregularities and nodular areas of the surface of the liver. The histological diagnosis of this patient was NASH stage 4, and the 3D-MR image of this patient is also shown in Fig. 1d.

In the present study, one patient was found to have hepatocellular carcinoma on MRI. However, the tumor was small (26 × 22 mm) and occupied a small proportion of the area of the entire surface of the liver; therefore, the diagnostic evaluation was not affected.

Diagnostic features of 3D-MRI and the APRI, FIB-4 index, and BARD scoring systems for advanced fibrosis of the liver

Table 2 summarizes the diagnostic features of 3D-MRI and each scoring system for advanced fibrosis. For the scoring systems (APRI, FIB-4 index, and BARD), the sensitivity ranged from 78 to 89 %, specificity from 71 to 90 %, PPV from 54 to 78 %, and NPV from 88 to 94 %. For 3D-MRI, the sensitivity was 100 %, specificity 90 %, PPV 82 %, and NPV 100 %.

Distributions of patients with advanced fibrosis of the liver according to 3D-MRI, APRI, FIB-4 index, and BARD, and histopathology

Figure 4 shows the distribution of patients predicted to have advanced fibrosis by 3D-MRI and each scoring system, along with the distribution of patients diagnosed with advanced fibrosis by histopathological evaluation. The scoring systems showed more varied distributions compared with 3D-MRI, which showed a uniform distribution that was similar to the histopathological distribution.

Discussion

Up to now, the definitive diagnosis of NASH has been based on histopathological evaluation. However, in Japan, many patients with NAFLD are diagnosed with NASH using US only, because liver biopsies have a risk of major complications such as intraperitoneal bleeding. However, some noninvasive scoring systems (APRI, BARD, and the FIB-4 index) for predicting fibrosis have become available [17]. In addition, the usefulness of other noninvasive strategies for predicting fibrosis in patients with NAFLD has been reported, including transient sonoelastography [21, 22], ARFI [23], and MR elastography [24]. However, these diagnostic methods may lack sensitivity for identifying advanced fibrosis. In addition, for the majority of patients with NAFLD, these methods of prediction usually have weak objectivity and persuasive power. Therefore, a more accurate noninvasive evaluation method is needed. In the present study, we described and reported on the use of "virtual MR-laparoscopy" for 3D imaging of the liver, or 3D-MRI. Although 3D-MRI has qualitative and subjective features, we found that it accurately predicted advanced fibrosis, because it could easily provide visualization of the entire surface of the liver, and evaluation was comparatively easy for physicians experienced with conventional diagnostic laparoscopy for chronic liver disease or treatment of hepatobiliary diseases such as cholecystolithiasis or hepatic tumor. In the present study, 3D-MRI demonstrated a high positive and negative predictive value for

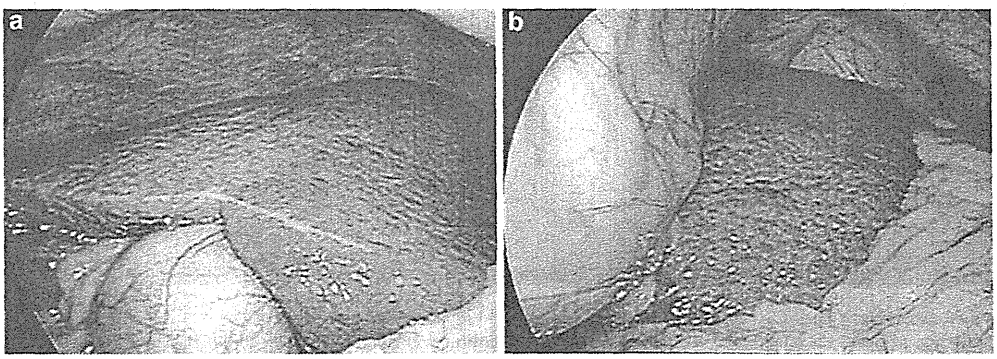

Fig. 2 Conventional laparoscopic image of the liver of the same patient in Fig. 1c. **a** View of the right lobe of the liver. The surface of the liver has diffuse small irregularities. **b** View of the left lobe of the liver. The surface of the liver has diffuse small irregularities and a large nodular area

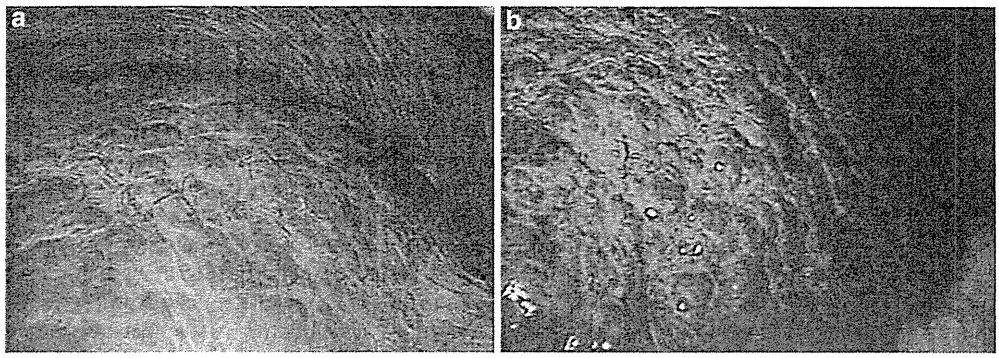

Fig. 3 Conventional laparoscopic image of the liver of the same patient in Fig. 1d. **a** View of the right lobe of the liver. The surface of the liver has diffuse large irregularities with nodular areas. **b** View of the left lobe of the liver. The surface of the liver has diffuse large irregularities with nodular areas

Table 2 Diagnostic features of three-dimensional magnetic resonance imaging and the APRI, FIB-4 index, and BARD scoring systems used to predict advanced liver fibrosis

	Sensitivity (%)	Specificity (%)	PPV (%)	NPV (%)
3D-MRI (virtual MR-laparoscopy)	100	90	82	100
APRI	78	71	54	88
FIB-4 index	78	90	78	90
BARD score	89	81	67	94

NPV negative predictive value, *PPV* positive predictive value

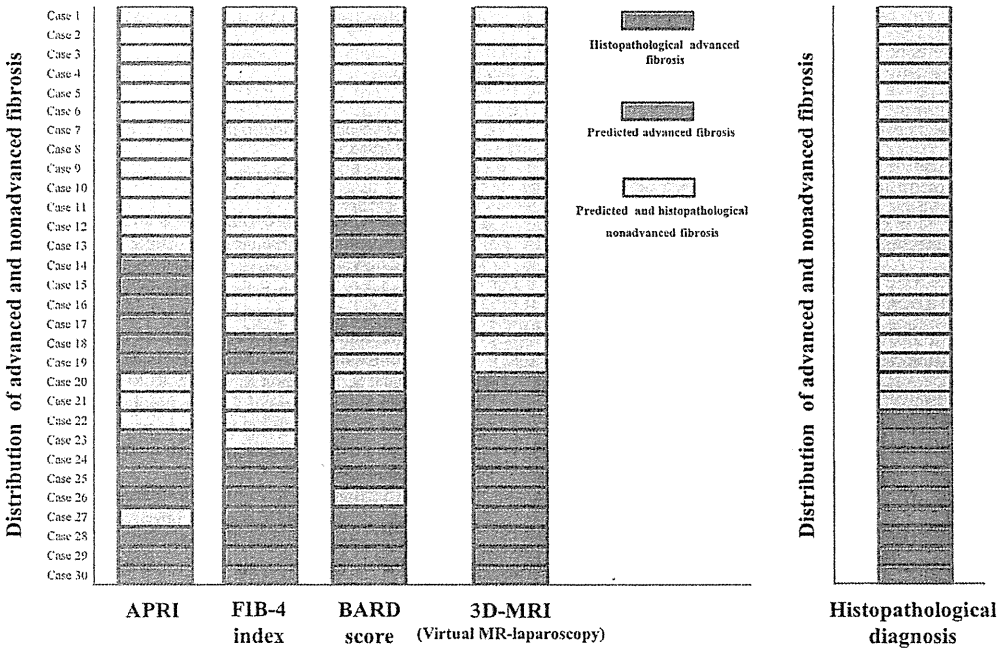

Fig. 4 Distribution of patients predicted to have advanced fibrosis by 3D-MRI and the APRI, FIB-4 index, and BARD scoring systems, along with the distribution of patients diagnosed with advanced fibrosis by histopathological evaluation

advanced fibrosis (82 and 100 %, respectively) and a sensitivity and specificity of 100 and 90 %, respectively.

We also evaluated the APRI, FIB-4 index, and BARD scoring systems, which are easy to calculate using three or four parameters that are routinely measured in outpatient medical practice. All these systems were found to have high predictive values for advanced fibrosis of the liver in this cohort. Figure 4 suggests that the combined use of 3D-MRI and a scoring system may be more advantageous for routine medical care than a single evaluation system. For example, it may be assumed that a double positive for advanced fibrosis provided by 3D-MRI and any one of the scoring systems would lead to a PPV increase from 82 to 90 %, while the NPV would remain 100 %.

However, there are some technical problems with 3D-MRI that still need to be resolved. Inadequate breath holding during the hepatobiliary phase leads to distorted hepatobiliary phase images and inaccurate findings. The 1.5-T MR-imaging system (Avanto) used for the patients in the present study required a 25-s breath hold; therefore, a patient with pulmonary emphysema might not be able to undergo this procedure. There is also the problem of motion artifact; the patients were all found to have linear surface irregularities where the superior border of the liver is near the inferior border of the heart. At present, the heart-beat-motion artifact is difficult to remove. Therefore, evaluation of liver surface irregularities seen on 3D-MRI should take into consideration the effect of the heart on the area of the liver below it. Both these problems may be resolved by increased high-speed image acquisition, which is based on the improvement of the signal-to-noise ratio resulting from the introduction of a powerful magnetic-field imaging system such as a 3.0-T MRI system and multichannel coil.

Despite the current technical problems of 3D-MRI, the large surface irregularities of liver cirrhosis associated with NASH (Fig. 1d) are easy to observe with this modality. However, the advanced fibrosis of NASH stage 3 usually manifests with small irregularities of the surface of the liver (Fig. 1c). Therefore, in patients with NASH stage 3, it is important to carefully examine the images for small irregularities, looking closely at the edge of the liver where the surface irregularities are most clearly depicted by 3D-MRI and clearly seen during conventional laparoscopy.

In the present study has some limitations. This was a retrospective cohort trial evaluating a small number of patients. There were a small number of patients because of the enrollment requirement that patients had to undergo 3D-MRI within 1 year before biopsy and histopathological evaluation. In addition, with regard to the liver biopsy specimens, there were significant differences in the length and number of portal areas of the specimens, and these differences may have led to underestimation of the extent of liver fibrosis in patients with nonadvanced fibrosis. Although in the present study there were no discrepancies among the three experienced hepatologists regarding the diagnosis of advanced fibrosis, 3D-MRI has qualitative and subjective features that might be affected by the different clinical experiences of physicians assessing the images derived from 3D-MRI. Because there were no methods for quantitative assessment of the surface irregularities of the liver seen on 3D-MRI, it was impossible to compare 3D-MRI with the other scoring systems by means of receiver-operating characteristic curve analysis. As stated above, the number of patients in the present study is too small, and some limitations have to be solved. In the near future, further additional large studies that include quantitative evaluation of the surface of the liver are needed.

However, we believe that the impact of the present study on the routine clinical care of patients with NAFLD, especially NASH patients, will be enormous. We also think that the progression of many high-risk patients to advanced liver disease, including decompensated liver cirrhosis and hepatocellular carcinoma, will be prevented by early detection of advanced fibrosis using 3D-MRI.

In conclusion, the diagnostic features of 3D-MRI for predicting advanced fibrosis associated with NASH were superior to those of other previously reported diagnostic methods.

Conflict of interest The authors state that they have no conflicts of interest regarding the content of the article.

Funding Okinaka Memorial Institute for Medical Research and Japanese Ministry of Health, Labour,and Welfare.

References

1. Angulo P. Nonalcoholic fatty liver disease. N Engl J Med. 2002;346:1221–1231
2. Williams R. Global changes in liver disease. Hepatology. 2006;44:521–526
3. Torres DM, Harrison SA. Diagnosis and therapy of nonalcoholic steatohepatitis. Gastroenterology. 2008;134:1682–1698
4. Vuppalanchi R, Chalasani N. Nonalcoholic fatty liver disease and nonalcoholic steatohepatitis: selected practical issues in their evaluation and management. Hepatology. 2009;49:306–317
5. Fan JG, Farrell GC. Epidemiology of non-alcoholic fatty liver disease in China. J Hepatol. 2009;50:204–210
6. Watanabe S, Yaginuma R, Ikejima K, Miyazaki A. Liver diseases and metabolic syndrome. J Gastroenterol. 2008;43:509–518
7. Adams LA, Lymp JF, St Sauver J, et al. The natural history of nonalcoholic fatty liver disease: a population-based cohort study. Gastroenterology. 2005;129:113–121
8. Ratziu V, Bonyhay L, Di Martino V, et al. Survival, liver failure, and hepatocellular carcinoma in obesity-related cryptogenic cirrhosis. Hepatology. 2002;35:1485–1493
9. Siegel AB, Zhu AX. Metabolic syndrome and hepatocellular carcinoma: two growing epidemics with a potential link. Cancer. 2009;115:1561–5651
10. Kawamura Y, Arase Y, Ikeda K, et al. Large-scale long-term follow-up study of Japanese patients with non-alcoholic fatty liver disease for the onset of hepatocellular carcinoma. Am J Gastroenterol. 2012;107:253–261

11. Kelling G. Zur Coelioskopie und Gastroskopie. Arch Klin Chir. 1923;126:226–229
12. Pagliaro L, Rinaldi F, Craxì A, et al. Percutaneous blind biopsy versus laparoscopy with guided biopsy in diagnosis of cirrhosis. A prospective, randomized trial. Dig Dis Sci. 1983;28:39–43
13. Helmreich-Becker I, Meyer zum Buschenfelde KH, Lohse AW. Safety and feasibility of a new minimally invasive diagnostic laparoscopy technique. Endoscopy. 1998;30:756–762
14. Ratziu V, Charlotte F, Heurtier A, LIDO Study Group, et al. Sampling variability of liver biopsy in nonalcoholic fatty liver disease. Gastroenterology. 2005;128:1898–906
15. Wai CT, Greenson JK, Fontana RJ, et al. A simple noninvasive index can predict both significant fibrosis and cirrhosis in patients with chronic hepatitis C. Hepatology. 2003;38:518–526
16. Sterling RK, Lissen E, Clumeck N, APRICOT Clinical Investigators, et al. Development of a simple noninvasive index to predict significant fibrosis in patients with HIV/HCV coinfection. Hepatology. 2006;43:1317–1325
17. Harrison SA, Oliver D, Arnold HL, Gogia S, Neuschwander-Tetri BA. Development and validation of a simple NAFLD clinical scoring system for identifying patients without advanced disease. Gut. 2008;57:1441–1447
18. Kruger FC, Daniels CR, Kidd M, et al. APRI: a simple bedside marker for advanced fibrosis that can avoid liver biopsy in patients with NAFLD/NASH. S Afr Med J. 2011;101:477–480
19. Vallet-Pichard A, Mallet V, Nalpas B, et al. FIB-4: an inexpensive and accurate marker of fibrosis in HCV infection. Comparison with liver biopsy and fibrotest. Hepatology. 2007;46:32–36
20. Shah AG, Lydecker A, Murray K, Nash Clinical Research Network, et al. Comparison of noninvasive markers of fibrosis in patients with nonalcoholic fatty liver disease. Clin Gastroenterol Hepatol. 2009;7:1104–1112
21. Yoneda M, Yoneda M, Mawatari H, et al. Noninvasive assessment of liver fibrosis by measurement of stiffness in patients with nonalcoholic fatty liver disease (NAFLD). Dig Liver Dis. 2008;40:371–378
22. Wong VW, Vergniol J, Wong GL, et al. Diagnosis of fibrosis and cirrhosis using liver stiffness measurement in nonalcoholic fatty liver disease. Hepatology. 2010;51:454–462
23. Yoneda M, Suzuki K, Kato S, et al. Nonalcoholic fatty liver disease: US-based acoustic radiation force impulse elastography. Radiology. 2010;256:640–647
24. Chen J, Talwalkar JA, Yin M, et al. Early detection of nonalcoholic steatohepatitis in patients with nonalcoholic fatty liver disease by using MR elastography. Radiology. 2001;259:749–756
25. Hammerstingl R, Huppertz A, Breuer J, European EOB-study group, et al. Diagnostic efficacy of gadoxetic acid (Primovist)-enhanced MRI and spiral CT for a therapeutic strategy: comparison with intraoperative and histopathologic findings in focal liver lesions. Eur Radiol. 2008;18:457–467
26. Hammerstingl R, Zangos S, Schwarz W, et al. Contrast-enhanced MRI of focal liver tumors using a hepatobiliary MR contrast agent: detection and differential diagnosis using Gd-EOB-DTPA-enhanced versus Gd-DTPA-enhanced MRI in the same patient. Acad Radiol. 2002;9(Suppl 1):S119–S120
27. Ward J. New MR techniques for the detection of liver metastases. Cancer Imag. 2006;6:33–42
28. Tanimoto A, Lee JM, Murakami T, et al. Consensus report of the 2nd International Forum for Liver MRI. Eur Radiol. 2009;19(Suppl 5):S975–S989
29. Huppertz A, Balzer T, Blakeborough A, European EOB Study Group, et al. Improved detection of focal liver lesions at MR imaging: multicenter comparison of gadoxetic acid-enhanced MR images with intraoperative findings. Radiology. 2004;230:266–275
30. Brunt EM, Janney CG, Di Bisceglie AM, Neuschwander-Tetri BA, Bacon BR. Nonalcoholic steatohepatitis: a proposal for grading and staging the histological lesions. Am J Gastroenterol. 1999;94:2467–2474
31. Ishak K, Baptista A, Bianchi L, et al. Histological grading and staging of chronic hepatitis. J Hepatol. 1995;22:696

Hepatology Research

Hepatology Research 2013; 43: 942–949 doi: 10.1111/hepr.12041

Original Article

Antitumor efficacy of transcatheter arterial chemoembolization with warmed miriplatin in hepatocellular carcinoma

Yuya Seko, Kenji Ikeda, Yusuke Kawamura, Taito Fukushima, Tasuku Hara, Hitomi Sezaki, Tetsuya Hosaka, Norio Akuta, Fumitaka Suzuki, Masahiro Kobayashi, Yoshiyuki Suzuki, Satoshi Saitoh, Yasuji Arase and Hiromitsu Kumada

Department of Hepatology, Toranomon Hospital, Tokyo, Japan

Aim: Patients with unresectable hepatocellular carcinoma (HCC) often undergo transcatheter arterial chemoembolization (TACE). Miriplatin is a lipophilic cisplatin derivative used in TACE that is effective in HCC. However, the difference in antitumor efficacy between warmed versus room temperature miriplatin is unclear.

Methods: Chemotherapy efficacy was evaluated by dynamic computed tomography 1–3 months after TACE, according to the Modified Response Evaluation Criteria in Solid Tumors. A total of 203 patients with HCC who received TACE with miriplatin for the first time were included in a follow-up study to retrospectively investigate its efficacy and safety. Overall, 45 patients underwent TACE with warmed (40°C) miriplatin and 158 patients received TACE with room temperature miriplatin.

Results: Seventy patients (44.3%) treated with room temperature miriplatin and 32 patients (71.1%) who received warmed miriplatin experienced complete or partial responses. Multivariate analysis identified miriplatin temperature (warmed miriplatin, risk ratio (RR) = 2.26, $P = 0.047$), tumor number (solitary, RR = 3.48, $P = 0.007$), α-fetoprotein (AFP) level (<50 ng/mL, RR = 2.35, $P = 0.012$) and history of TACE (no history, RR = 2.22, $P = 0.041$) as predictors of objective response following TACE with miriplatin, and no serious complications were observed.

Conclusion: Warm temperature, solitary tumors, low AFP level and first TACE are significant and independent predictors of objective response after TACE using miriplatin. These results suggest that warmed miriplatin can be considered as one of the standard treatments for unresectable HCC.

Key words: hepatocellular carcinoma, miriplatin, transcatheter arterial chemoembolization

INTRODUCTION

HEPATOCELLULAR CARCINOMA (HCC) is one of the most common malignant diseases worldwide.[1] In Japan, more than 30 000 people die of HCC each year, and HCC ranks third and fifth in men and women, respectively, as cause of death due to malignant neoplasms.[2] Because resection, liver transplantation and percutaneous ablation (percutaneous ethanol injection and radiofrequency ablation) are applicable in only 30–40% of HCC patients, transcatheter arterial chemoembolization (TACE) has been recognized as an effective palliative treatment option for patients with advanced HCC.[3–10] TACE is recommended for HCC patients with class A or B liver damage, two or three tumors, and a tumor diameter greater than 3 cm, according to the guidelines for treatment of HCC by the Japan Society of Hepatology in 2009.[11] The Barcelona Clinic Liver Cancer group recommends TACE for HCC patients with stage B and class A or B disease and more than four tumors, or stage C disease without portal vein invasion or extrahepatic metastasis.[12] Miriplatin (cis-[1R,2R]-1,2-cyclohexanediamine-N,N']bis[myristate])-platinum(II) monohydrate; Dainippon Sumitomo Pharma, Osaka, Japan) is a novel lipophilic cisplatin derivative that can be suspended in lipiodol, a lipid lymphographic agent.[13–16] Some trials reported that miriplatin is effective for HCC.[17,18] Addition of embolizing agents to miriplatin-based treatment has been shown to result in a higher response in patients with

Correspondence: Dr Yuya Seko, Department of Hepatology, Toranomon Hospital, 2-2-2 Toranomon, Minato-ku, Tokyo 105-0001, Japan. Email: yseko523@toranomon.gr.jp
Received 26 August 2012; revision 11 November 2012; accepted 3 December 2012.

HCC.[19] Significant predictors for complete response to miriplatin include solitary tumors, previous complete response to TACE via injection from the peripheral to segmental hepatic artery,[20] and stage I or II disease.[21] The most important issue regarding TACE with miriplatin is its viscosity: due to its high viscosity, miriplatin/lipiodol suspension cannot enter smaller vessels. We previously determined that warming miriplatin to 40°C decreased its viscosity in vitro (unpubl. obs.). We investigated the viscosity of miriplatin/lipiodol suspension using a viscometer (μVISC; RHEOSENSE, San Ramon, CA, USA). The miriplatin/lipiodol suspension was adjusted to 20 mg/mL, and then warmed to 40°C. We measured the viscosity of these solutions at room temperature and 40°C three times, and determined that the mean viscosity of miriplatin/lipiodol suspension at room temperature and 40°C is 37.48 mPa-S and 21.42 mPa-S, respectively. The purpose of this retrospective study was to evaluate the antitumor efficacy and adverse effects of TACE with warmed miriplatin suspension.

METHODS

Patients

A TOTAL OF 402 HCC Japanese adult patients were consecutively recruited into the study protocol of TACE with miriplatin from December 2007 to June 2012 at our center. Among them, 203 patients who received miriplatin for the first time and who were assessed 1–3 months after TACE were enrolled in this retrospective study. Warmed miriplatin was used for all patients from August 2011 to June 2012. Overall, 45 patients received warmed miriplatin and 158 patients received room temperature miriplatin.

Table 1 summarizes the profile and laboratory data of the study patients. The median follow-up period, from the end of TACE until the last visit, was 458 days (range, 57–1226 days). Higher serum aspartate aminotransferase (AST) levels and prothrombin activity were observed in patients in the room temperature miriplatin group compared to those in the warmed miriplatin group. The study protocol was approved by the ethics committee of our hospital, and written informed consent was obtained from all participating patients.

HCC

Before treatment with miriplatin, all patients underwent a comprehensive evaluation consisting of a medical history, physical examination, measurement of tumor size, performance status, chest radiograph, liver-imaging studies (dynamic computed tomography [CT], ultrasonography [US], digital-subtraction angiography [DSA]), complete blood count and blood chemistry. Diagnosis of HCC was established based on the findings

Table 1 Profile and pretreatment laboratory data of 203 patients who underwent TACE using miriplatin/lipiodol suspension under room temperature and warmed conditions for unresectable HCC

	Total	Room temperature miriplatin group	Warmed miriplatin group	*P*-value
Demographic data				
No. of patients	203	158	45	
Sex (male/female)	130/73	99/59	31/14	0.485
Age, years†	73 (45–91)	71 (45–91)	74 (48–86)	0.940
Etiology, HBV/HCV/other	24/161/18	17/130/11	7/31/7	0.097
Laboratory data†				
Albumin, g/dL	3.0 (2.0–4.2)	3.3 (2.0–4.2)	3.0 (2–4.1)	0.553
Serum aspartate aminotransferase, IU/L	50 (18–415)	52 (18–415)	47 (19–305)	0.033
Serum alanine aminotransferase, IU/L	34 (12–282)	34 (12–171)	31 (12–282)	0.311
Total bilirubin, mg/dL	1.0 (0.4–4.9)	1.1 (0.4–4.9)	1.0 (0.4–2.7)	0.902
Platelet count, $\times 10^3/mm^3$	9.6 (1.9–28.2)	9.5 (1.9–28.2)	10.0 (3.5–26.5)	0.716
Prothrombin activity, %	79.2 (40.8–123.1)	81.5 (45.7–123.1)	74.0 (40.8–106.1)	0.005
AFP, μg/L	30.0 (1.8–282 200)	32.3 (1.8–282 200)	22.0 (2.9–49 710)	0.527
AFP-L3, %	19.0 (0–82.7)	22.7 (0–82.7)	12.0 (0–78.0)	0.601
DCP, AU/L	39.0 (4–662 000)	40.5 (4–65 290)	30 (8–662 000)	0.748
Child–Pugh class, A/B	152/51	119/39	33/12	0.846

Data are shown as number and percentage of patients, except those denoted by †, which represent the median (range) values.
AFP, α-fetoprotein; AFP-L3, *Lens culinaris* agglutinin-reactive fraction of AFP; DCP, des-γ-carboxy prothrombin; HBV, hepatitis B virus; HCC, hepatocellular carcinoma; HCV, hepatitis C virus; TACE, transcatheter arterial chemoembolization.

of dynamic CT, US and DSA. Patients who had extrahepatic metastasis of HCC or other malignancies were excluded.

Table 2 summarizes the tumor profiles and TACE treatment history of patients in each study group. In the warmed miriplatin group, 12 patients (26.7%) had a solitary tumor and 33 patients (73.3%) had multiple tumors. The median diameter of the largest tumor was 30 mm (range, 6–115 mm) and 29 patients (64.4%) had a history of TACE. In the room temperature miriplatin group, 29 patients (18.4%) had a solitary tumor and 129 patients (81.6%) had multiple tumors. The median diameter of the largest tumor was 30 mm (range, 6–125 mm), and 120 patients (75.9%) had a history of TACE. Patients in the room temperature miriplatin group tended to have more tumors than those in the warmed miriplatin group.

Treatment protocol

Patients were hydrated through a peripheral line. The femoral artery was catheterized under local anesthesia, and a 4-Fr Shepherd Hook catheter (FansacIV or Angiomaster; Terumo Clinical Supply, Gifu, Japan) was inserted into the hepatic artery, and portography through the superior mesenteric artery and celiac arteriography were performed. Then, a 2.0- or 2.1-Fr microcatheter was advanced into the feeding arteries of each tumor, and miriplatin suspended in lipiodol solution was injected into the hepatic artery; however, the injection was discontinued immediately before the flow ceased completely. Thereafter, the feeding arteries to the tumors were embolized with 1-mm gelatin cubes (Gelpart; Nippon Kayaku, Tokyo, Japan). The miriplatin/lipiodol suspension was administrated slowly under careful fluoroscopic guidance. The dose of miriplatin/lipiodol was 120–180 mg/2–3 mL and was determined based on tumor size and degree of liver dysfunction. A 5-HT3 antagonist was administrated before the miriplatin injection; however, hydration by i.v. fluid administration was not conducted before the TACE procedure. A clean container was placed in an electric range filled with water. The injector of miriplatin/lipiodol suspension and sterilized physiological saline were then placed in the container, and the container was warmed to 60°C. We observed that in 60°C water, the miriplatin/lipiodol suspension in the injector reaches 40°C *in vitro*. The stability of warmed miriplatin/lipiodol suspension has been previously reported.

Assessment of therapeutic efficacy

The efficacy of chemotherapy was evaluated by dynamic CT 1–3 months after TACE with miriplatin, and was based on change in the maximum diameter of viable target lesions (i.e. those showing enhancement in the arterial phase). Response categories, according to the Modified Response Evaluation Criteria in Solid Tumors[22] are as follows: complete response (CR), disappearance of any intratumoral arterial enhancement in all target lesions; partial response (PR), at least a 30% decrease in the sum of diameters of viable target lesions; stable disease (SD), any cases that do not qualify for either PR or progressive disease; and progressive disease (PD), an increase of at least 20% in the sum of the diameters of viable target lesions.

Toxicity evaluation

Treatment-related toxicity was assessed using the National Cancer Institute Common Terminology Criteria (ver. 4.0). Within 2 weeks before TACE with miriplatin, and at 3–7 days (three times during this period) and at 1 month afterward, hematological (i.e. leukocyte and thrombocyte counts) and clinical chemistry (i.e. serum AST, serum alanine aminotransferase [ALT],

Table 2 Tumor profile and treatment history of 203 patients who underwent TACE using miriplatin/lipiodol suspension under room temperature condition and warmed conditions for unresectable HCC

	Total	Room temperature miriplatin group	Warmed miriplatin group	*P*-value
No. of patients	203	158	45	
Tumor size, mm†	20 (6–125)	30 (6–125)	30 (6–115)	0.435
Tumor multiplicity (solitary/multiple)	41/162	29/129	12/33	0.291
No. of tumors†	3 (1–100)	3 (1–100)	3 (1–40)	0.030
Stage (I/II/III/IV)	54/81/66/2	38/67/51/2	16/14/15/0	0.329
History of TACE	73.4%	75.9%	64.4%	0.130

Data are shown as number and percentage of patients, except those denoted by †, which represent the median (range) values.
HCC, hepatocellular carcinoma; TACE, transcatheter arterial chemoembolization.

albumin, total bilirubin, serum creatine and prothrombin activity) toxicity evaluations were conducted.

Statistical analysis

The distribution of subject characteristics was assessed by the χ^2-test or Mann–Whitney *U*-test, as appropriate. Logistic analysis was used to determine independent predictive factors associated with CR and PR by TACE with miriplatin. The risk ratio (RR) and 95% confidence interval (CI) were also calculated. Variables that achieved statistical significance ($P < 0.05$) or marginal significance ($P < 0.10$) on univariate analysis were entered into a multivariate Cox proportional hazard model to identify significant independent factors. Statistical comparisons were performed using SPSS software (SPSS, Chicago, IL, USA). All *P*-values of less than 0.05 by two-tailed test were considered significant.

RESULTS

Treatment effects

OF THE 203 treated patients, 55 (27.1%) experienced a CR, 47 patients (23.2%) PR, 66 patients (32.5%) SD and 33 patients (17.2%) PD. Overall, 50.3% of patients achieved an objective response (i.e. CR plus PR).

Predictive factors associated with objective response to TACE

Data from the entire study population were analyzed to identify factors that could predict objective response. Univariate analysis identified five parameters that tended to correlate or significantly correlated with objective response: miriplatin temperature (warmed miriplatin, $P = 0.002$), tumor number (solitary tumor, $P < 0.001$), α-fetoprotein (AFP) level (<50 ng/mL, $P = 0.003$), *Lens culinaris* agglutinin-reactive fraction of AFP (AFP-L3%) (<10%, $P = 0.032$) and history of TACE (no history, $P = 0.002$). These five factors were entered into multivariate analysis, which revealed four parameters to be significant and independent determinants of objective response using miriplatin: miriplatin temperature (warmed miriplatin, risk ratio [RR] = 2.26, $P = 0.047$), tumor number (solitary tumor, RR = 3.48, $P = 0.007$), AFP level (<50 ng/mL, RR = 2.35, $P = 0.012$) and history of TACE (no history, RR = 2.22, $P = 0.041$) (Table 3).

Objective response according to AFP-L3%

Patients were divided into two groups according to AFP-L3 serum level using a cut-off value of 10% (low AFP-L3 group [<10%], $n = 83$; high AFP-L3 group [≥10%], $n = 89$). In the high AFP-L3 group, 27 of 83 patients (32.5%) experienced CR, 22 patients (26.5%) PR, 26 patients (31.3%) SD and eight patients (9.6%) PD. In the low AFP-L3 group, 17 of 89 patients (19.1%) experienced CR, 20 patients (22.5%) PR, 29 patients (32.6%) SD and 23 patients (25.8%) PD. The response rates were significantly different between the two groups ($P = 0.032$, log-rank test).

Objective response according to miriplatin temperature, tumor number, AFP and history of TACE

Next, the efficacy of TACE using miriplatin according to temperature condition was examined (Fig. 1). In the warmed miriplatin group, 19 of 45 patients (42.2%) experienced CR, 13 patients (28.9%) PR, eight patients (17.8%) SD and five patients (11.1%) PD. In the room temperature miriplatin group, 36 of 158 patients (22.8%) experienced CR, 34 patients (21.5%) PR, 58

Table 3 Factors associated with objective response (CR plus PR) after TACE using miriplatin, identified by multivariate analysis

Factors	Category	Risk ratio (95% confidence interval)	*P*-value†
Miriplatin condition	1: Room temperature	1	0.047
	2: Warmed	2.26 (1.01–5.04)	
Tumor number	1: Multiple nodules	1	0.007
	2: Solitary nodule	3.48 (1.42–8.62)	
AFP	1: ≥50 ng/mL	1	0.012
	2: <50 ng/mL	2.35 (1.21–4.57)	
History of TACE	1: Yes	1	0.041
	2: No	2.22 (1.03–4.75)	

†Cox proportional hazard model.
AFP, α-fetoprotein; CR, complete response; PR, partial response; TACE, transcatheter arterial chemoembolization. [Correction made after online publication on 14 March 2013: Category 1 of AFP was changed to ≥50 ng/mL, and category 2 of AFP was changed to <50ng/mL.]

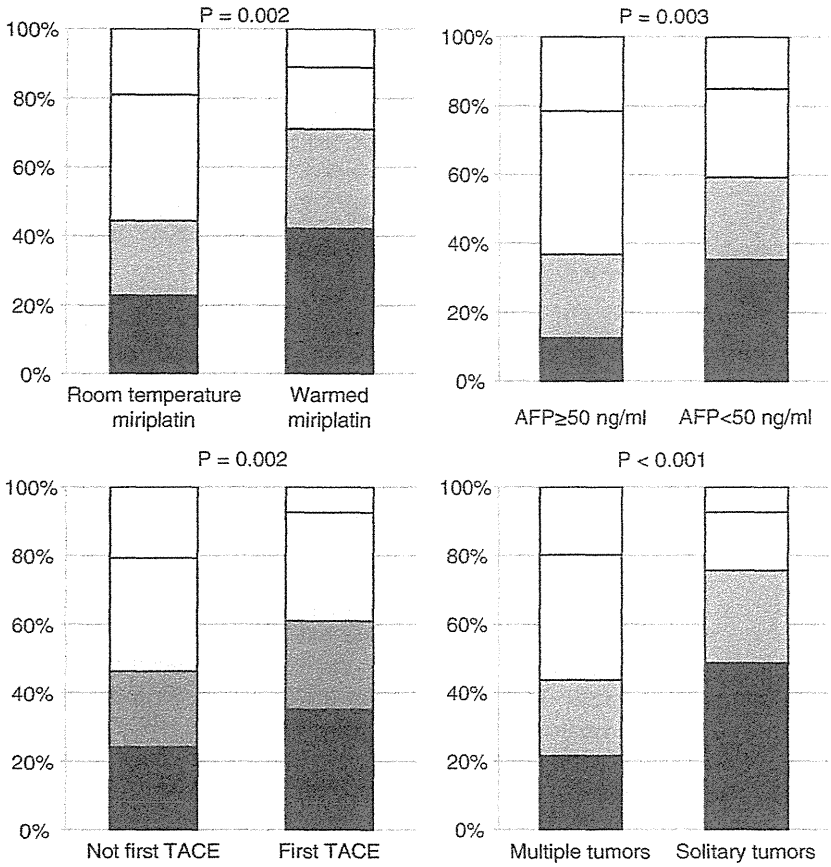

Figure 1 Efficacy of transcatheter arterial chemoembolization (TACE) using miriplatin in patients with hepatocellular carcinoma according to miriplatin temperature, serum α-fetoprotein (AFP) level, history of TACE and tumor number. Complete response (CR) and partial response (PR) rates were significantly higher for patients who received warmed miriplatin, had a low AFP level, were undergoing their first TACE and/or had solitary tumors. □, progressive disease (PD); ▨, stable disease (SD); ▩, PR; ■, CR. [Correction made after online publication on 14 March 2013: In the history of TACE diagram, the left column was relabeled as 'Not first TACE' while the right column was relabeled as 'First TACE'.]

patients (36.7%) SD and 30 patients (19.0%) PD. Overall, 71.1% of patients in the warmed miriplatin group and 44.3% of patients in the room temperature miriplatin group experienced an objective response (i.e. CR plus PR). The rates were significantly different between the two groups ($P = 0.002$, log-rank test).

In the high AFP group (≥50 ng/mL, $n = 79$), 10 of 79 patients (12.7%) experienced CR, 19 patients (24.1%) PR, 33 patients (41.8%) SD and 17 patients (21.5%) PD. In the low AFP group (<50 ng/mL, $n = 113$), 40 of 113 patients (35.4%) experienced CR, 27 patients (23.9%) PR, 29 patients (25.7%) SD and 17 patients (15.0%) PD (Fig. 1). The rates were significantly different between the two groups ($P = 0.003$, log-rank test).

In the TACE-naïve group ($n = 54$), 19 of 54 patients (35.2%) experienced CR, 14 patients (25.9%) PR, 17 patients (31.5%) SD and four patients (7.4%) PD. In patients who had previously undergone TACE ($n = 149$), 36 of 149 patients (24.2%) experienced CR, 33 patients (22.1%) PR, 49 patients (32.9%) SD and 31 patients (20.8%) PD (Fig. 1). The rates were significantly different between the two groups ($P = 0.002$, log-rank test).

Among all patients, 41 patients (20.2%) had a solitary tumor and 162 (79.8%) had multiple tumors. In the solitary tumor group, 20 of 41 treated patients (48.8%) experienced CR, 11 patients (26.8%) PR, seven patients (17.1%) SD and three patients (7.3%) PD. In the multiple tumors group, 35 of 162 patients (21.6%) experienced CR, 36 patients (22.2%) PR, 59 patients (36.4%) SD and 32 patients (19.8%) PD (Fig. 1). The rates were significantly different between the two groups ($P < 0.001$, log-rank test).

Adverse effects

Fever, anorexia and elevated serum transaminase levels were observed in most patients after miriplatin administration (Table 4). In the room temperature miriplatin group and warmed miriplatin groups, the following grade 4 events were observed: increased AST in four

Table 4 Adverse effects following miriplatin administration

	Room temperature condition ($n = 158$)				Warmed condition ($n = 45$)			
	Grade 1	Grade 2	Grade 3	Grade 4	Grade 1	Grade 2	Grade 3	Grade 4
White blood cells decreased	11 (7.0%)	19 (12.0%)	1 (0.6%)	0	5 (10.7%)	4 (8.9%)	0	0
Anemia	96 (60.8%)	19 (12.0%)	5 (3.2%)	0	21 (46.7%)	6 (17.9%)	0	0
Platelet count decreased	80 (50.6%)	38 (24.1%)	20 (12.7%)	0	22 (48.9%)	10 (22.2%)	3 (6.7%)	0
Aspartate aminotransferase increased	75 (47.5%)	33 (20.9%)	38 (24.1%)	4 (2.5%)	21 (46.7%)	7 (15.6%)	20 (28.6%)	2 (4.4%)
Alanine aminotransferase increased	74 (46.8%)	17 (10.8%)	22 (13.9%)	1 (0.6%)	21 (46.7%)	10 (22.2%)	4 (8.9%)	2 (4.4%)
Fever	72 (45.6%)	17 (10.8%)	0	0	22 (48.9%)	7 (17.9%)	0	0
Appetite loss	63 (39.9%)	2 (1.3%)	0	0	25 (55.6%)	0	0	0
Abdominal pain	30 (0.6%)	5 (3.2%)	0	0	4 (10.7%)	2 (4.4%)	0	0

Values denote numbers of subjects. Treatment-related toxicity was assessed using the National Cancer Institute Common Terminology Criteria ver. 4.0.

(2.5%) and one patient (3.5%), respectively, and increased ALT in one (0.6%) and one patient (3.6%), respectively; all of these elevations resolved within 2 weeks. No vascular complications of the hepatic artery were observed in any patient. No other serious complications or treatment-related deaths were observed following miriplatin administration. No significant differences in adverse effects were observed between the two groups.

DISCUSSION

TRANSCATHETER ARTERIAL CHEMOEMBOLIZATION is widely performed in patients with HCC who are not eligible for curative therapy. Previous randomized controlled trials and meta-analyses confirmed the survival benefit of TACE. Because many anticancer drugs, such as doxorubicin, epirubicin, mitomycin C, cisplatin and neocarzinostatin, have been used for the treatment of HCC, the most effective and least toxic agents or protocol remain unclear.[23,24] In most patients, TACE can be repeated, and using the same agent multiple times can lead to resistance. A previous study reported that platinum analogs are frequently effective for advanced HCC that are unresponsive to TACE with epirubicin.[25] Miriplatin was developed as a lipophilic platinum complex that has superior antitumor efficacy in HCC with lower toxicity compared to cisplatin.[13–16] Previous reports suggested that TACE with miriplatin can be used safely for HCC patients with chronic renal failure.[26]

Pharmacokinetic studies have demonstrated that the plasma concentration of total platinum is much lower in patients treated with miriplatin compared with that in patients treated with intra-arterial cisplatin: the C_{max} is approximately 300-fold lower and the T_{max} roughly 500-fold longer for miriplatin than the corresponding values for intra-arterial cisplatin. Miriplatin/lipiodol suspension is a stable colloidal emulsion that is deposited within HCC tumors, where it gradually releases active derivatives of miriplatin. Miriplatin/lipiodol releases 1,2-diaminocyclohexane platinum (II) dichloride (DPC) as its active platinum compound, which binds to nuclear DNA and mediates miriplatin/lipiodol cytotoxicity. In a cisplatin-resistant rat hepatoma cell line model, cross-resistance to DPC was not observed.[27]

Previous studies reported the efficacy of miriplatin, but differences in efficacy associated with miriplatin temperature have not yet been evaluated. In the present study, we examined predictors of objective response to TACE with miriplatin. Multivariate analysis identified

use of warmed miriplatin, low serum AFP, first TACE and solitary tumors as predictors of objective response in patients who received TACE with miriplatin. Previous reports identified CR after previous TACE, solitary tumor, injection from peripheral to segmental hepatic artery,[20] and stage I or II disease[21] as significant predictors associated with CR to TACE with miriplatin. Another report stated that the rates of local recurrence and intratumoral recurrence in patients treated with epirubicin were significantly lower than those in patients treated with miriplatin.[28] In the present study, some of the above factors were not identified as significant predictors of response. The differences in the findings of the present study and the reports described above are not currently clear, but may reflect differences in the population samples, as this was the first study to focus on the objective response of patients receiving miriplatin for the first time. Notably, the present study is the first study to investigate the viscosity of miriplatin/lipiodol suspension. Further studies of larger populations including individuals of other ethnicities are necessary.

In this study, warmed miriplatin was associated with objective response after TACE. The main issue associated with miriplatin administration is its high viscosity, which prevents the miriplatin/lipiodol suspension from flowing into the peripheral artery and leads to inhomogeneous distribution of miriplatin/lipiodol suspension in HCC tumors. This is the primary reason that TACE with miriplatin is associated with reduced efficacy compared to TACE with other agents.[28] Basic research has provided evidence that as the temperature of miriplatin/lipiodol suspension rises, its viscosity decreases; for example, the viscosity of miriplatin/lipiodol suspension at 40°C is 0.51-times that at 25°C. The chemical behavior of miriplatin does not change until its temperature reaches 70°C. Further studies should be performed to investigate the viscosity and antitumor efficacy of condensed and warmed miriplatin conditions, as well as the associated wash-out periods. In addition, although no significant differences in adverse effects between groups were noted, further follow up regarding vascular complications of the hepatic artery is required.

Previous studies reported the relationship between tumor multiplicity and efficacy of TACE.[20] TACE can be performed selectively, and the dose of drug per tumor is higher in patients with solitary tumors than in those with multiple tumors. In the present study, solitary tumors and warmed miriplatin were associated with objective response. These results are not inconsistent with previous studies. Interestingly, in the present patients, the impact of warmed miriplatin and solitary tumor was more significant than that of age, liver function, tumor size, tumor stage, tumor markers, injection artery and history of TACE. One possible explanation for this finding is that the study population included patients who received TACE with miriplatin for the first time. Previous studies reported that complete tumor necrosis after TACE offered favorable long-term survival outcomes in HCC patients.[5,29] In the current study, warmed miriplatin administration was associated with objective response, suggesting that warmed miriplatin administration potentially results in a favorable prognosis for HCC.

The present study has certain limitations. This was a retrospective study and the patients were not randomized with respect to treatment with warmed versus room temperature miriplatin. A prospective study is needed to assess the safety and efficacy of warmed miriplatin administration. The other limitation is the small number of cases in the warmed miriplatin group. A study with a larger number of patients is required to confirm the present results. Furthermore, evaluation of the efficacy of warmed miriplatin compared with epirubicin or cisplatin in HCC is also required.

In conclusion, the present study identified warmed miriplatin and solitary tumors as significant and independent predictors of objective response after TACE using miriplatin. The results emphasize the importance of the condition under which miriplatin is administrated, and we recommend that warmed miriplatin should be the standard method of administration for patients with unresectable HCC undergoing TACE.

ACKNOWLEDGMENTS

THIS STUDY WAS supported in part by a Grant-in-Aid from the Ministry of Health, Labor and Welfare, Japan.

REFERENCES

1 Parkin DM, Bray F, Ferlay J, Pisani P. Global cancer statistics, 2002. *CA Cancer J Clin* 2005; 55: 74–108.
2 Umemura T, Ichijo T, Yoshizawa K, Tanaka E, Kiyosawa K. Epidemiology of hepatocellular carcinoma in Japan. *J Gastroenterol* 2009; 44 (Suppl): 102–7.
3 Yamada R, Sato M, Kawabata M, Nakatsuka H, Nakamura K, Takashima S. Hepatic artery embolization in 120 patients with unresectable hepatoma. *Radiology* 1983; 148: 397–401.
4 Lin DY, Liaw YF, Lee TY, Lai CM. Hepatic arterial embolization in patients with unresectable hepatocellular carcinoma: a randomized controlled trial. *Gastroenterology* 1988; 94: 453–6.

5 Ikeda K, Kumada H, Saitoh S, Arase Y, Chayama K. Effect of repeated transcatheter arterial embolization on the survival time in patients with hepatocellular carcinoma. *Cancer* 1991; 68: 2150–4.
6 Llovet JM, Real MI, Montana X *et al.*; Barcelona Liver Cancer Group. Arterial embolisation or chemoembolization versus symptomatic treatment in patients with unresectable hepatocellular carcinoma: a randomised controlled trial. *Lancet* 2002; 359: 1734–9.
7 Lo CM, Ngan H, Tso WK *et al.* Randomized controlled trial of transarterial lipiodol chemoembolization for unresectable hepatocellular carcinoma. *Hepatology* 2002; 35: 1164–71.
8 Camma C, Schepis F, Orlando A *et al.* Transarterial chemoembolization for unresectable hepatocellular carcinoma: meta-analysis of randomized controlled trials. *Radiology* 2002; 224: 47–54.
9 Ikeda M, Maeda S, Shibata J *et al.* Transcatheter arterial chemotherapy with and without embolization in patients with hepatocellular carcinoma. *Oncology* 2004; 66: 24–31.
10 Takayasu K, Arii S, Ikai I *et al.*; Liver Cancer Study Group of Japan. Prospective cohort study of transarterial chemoembolization for unresectable hepatocellular carcinoma in 8510 patients. *Gastroenterology* 2006; 131: 461–9.
11 Arii S, Sata M, Sakamoto M *et al.* Management of hepatocellular carcinoma: report of consensus meeting in the 45th annual meeting of the Japan Society of Hepatology (2009). *Hepatol Res* 2010; 40: 667–85.
12 Bruix J, Sala M, Llovet JM. Chemoembolization for hepatocellular carcinoma. *Gastroenterology* 2004; 127 (5 Suppl 1): S179–S188.
13 Maeda M, Uchida NA, Sasaki T. Liposoluble platinum (II) complexes with antitumor activity. *Jpn J Cancer Res* 1986; 77: 523–5.
14 Kishimoto S, Ohtani A, Fukuda H, Fukushima S, Takeuchi Y. Relation between intracellular accumulation and cytotoxic activity of cis-[((1R,2R)-1, 2-cyclohexanediamine- N, N')bis(myristato)]platinum(II) suspended in Lipiodol. *Biol Pharm Bull* 2003; 26: 683–6.
15 Hanada M, Baba A, Tsutsumishita Y, Noguchi T, Yamaoka T. Intra-hepatic arterial administration with miriplatin suspended in an oily lymphographic agent inhibits the growth of human hepatoma cells orthotopically implanted in nude rats. *Cancer Sci* 2009; 100: 189–94.
16 Hanada M, Baba A, Tsutsumishita Y *et al.* Intra-hepatic arterial administration with miriplatin suspended in an oily lymphographic agent inhibits the growth of tumors implanted in rat livers by inducing platinum-DNA adducts to form and massive apoptosis. *Cancer Chemother Pharmacol* 2009; 64: 473–83.
17 Fujiyama S, Shibata J, Maeda S *et al.* Phase I clinical study of a novel lipophilic platinum complex (SM-11355) in patients with hepatocellular carcinoma refractory to cisplatin/lipiodol. *Br J Cancer* 2003; 89: 1614–19.
18 Okusaka T, Okada S, Nakanishi T, Fujiyama S, Kubo Y. Phase II trial of intra-arterial chemotherapy using a novel lipophilic platinum derivative (SM-11355) in patients with hepatocellular carcinoma. *Invest New Drugs* 2004; 22: 169–76.
19 Imai N, Ikeda K, Kawamura Y *et al.* Transcatheter arterial chemotherapy using miriplatin-lipiodol suspension with or without embolization for unresectable hepatocellular carcinoma. *Jpn J Clin Oncol* 2012; 42: 175–82.
20 Imai N, Ikeda K, Seko Y *et al.* Previous chemoembolization response after transcatheter arterial chemoembolization (TACE) can predict the anti-tumor effect of subsequent TACE with miriplatin in patients with recurrent hepatocellular carcinoma. *Oncology* 2011; 80: 188–94.
21 Imai Y, Chikayama T, Nakazawa M *et al.* Usefulness of miriplatin as an anticancer agent for transcatheter arterial chemoembolization in patients with unresectable hepatocellular carcinoma. *J Gastroenterol* 2011 [Epub ahead of print].
22 Lencioni R, Llovet JM. Modified RECIST (mRECIST) assessment for hepatocellular carcinoma. *Semin Liver Dis* 2010; 30: 52–60.
23 Marelli L, Stigliano R, Triantos C *et al.* Transarterial therapy for hepatocellular carcinoma: which technique is more effective? A systematic review of cohort and randomized studies. *Cardiovasc Intervent Radiol* 2007; 30: 6–25.
24 Kamada K, Nakanishi T, Kitamoto M *et al.* Long-term prognosis of patients undergoing transcatheter arterial chemoembolization for unresectable hepatocellular carcinoma: comparison of cisplatin lipiodol suspension and doxorubicin hydrochloride emulsion. *J Vasc Interv Radiol* 2001; 12: 847–54.
25 Kawamura Y, Ikeda K, Hirakawa M *et al.* Efficacy of platinum analogue for advanced hepatocellular carcinoma unresponsive to transcatheter arterial chemoembolization with epirubicin. *Hepatol Res* 2009; 39: 346–54.
26 Imai N, Ikeda K, Seko Y *et al.* Transcatheter arterial chemotherapy with miriplatin for patients with hepatocellular carcinoma and chronic renal failure. *Nihon Shokakibyo Gakkai Zasshi* 2011; 108: 1872–8.
27 Kishimoto S, Miyazawa K, Terakawa Y *et al.* Cytotoxicity of cis-[((1R,2R)-1,2-cyclohexanediamine-N,N')bis (myristato)]-platinum (II) suspended in Lipiodol in a newly established cisplatin-resistant rat hepatoma cell line. *Jpn J Cancer Res* 2000; 91: 1326–32.
28 Miyayama S, Yamashiro M, Shibata Y *et al.* Comparison of local control effects of superselective transcatheter arterial chemoembolization using epirubicin plus mitomycin C and miriplatin for hepatocellular carcinoma. *Jpn J Radiol* 2012; 30: 263–70.
29 Shim JH, Kim KM, Lee YJ *et al.* Complete necrosis after transarterial chemoembolization could predict prolonged survival in patients with recurrent intrahepatic hepatocellular carcinoma after curative resection. *Ann Surg Oncol* 2010; 17: 869–77.